A modeling study of the nighttime equatorial *E* region behavior during magnetospheric substorms and storms

V. P. Kim and V. V. Hegai
IZMIRAN, Troitsk, Moscow Region, Russia

M. Lal
Equatorial Geophysical Research Laboratory, Indian Institute of Geomagnetism, Krishnapuram, Tirunelveli, India

Received 5 March 2001; revised 10 October 2001; accepted 10 October 2001; published 28 May 2002.

[1] The results of a modeling study of the variations of altitude ion density distribution in the nighttime *E* region over the magnetic equator during strong magnetospheric substorms and storms due to perturbations of the zonal electric field E_y are presented. The ion density N is calculated by solving the time-dependent continuity equation for ion density by assuming the time variations of E_y, which are fitted to some of the observed ones. It is shown that during severe magnetospheric disturbances, the altitude structure of the nighttime equatorial *E* region is substantially modified, with the largest effects in the lower part of *E* region ($z < 105$ km), where a deep trough in ion density is formed instead of the quiet *E* region maximum. The ion density in the trough can be $\sim$1/6 times the undisturbed value of N. The *E* region maximum N_mE can be lifted up by $\sim$30 km, being $\sim 2\times$ decreased as compared with the quiet time value of N_mE. In the course of the magnetospheric disturbance the *E* region is bifurcated into two layers. *INDEX TERMS:* 2411 Ionosphere: Electric fields (2712); 2415 Ionosphere: Equatorial ionosphere; 2431 Ionosphere: Ionosphere/magnetosphere interactions (2736); *KEYWORDS:* storm and substorms, equatorial ionosphere, electric fields, ionospheric disturbances

1. Introduction

[2] The equatorial ionosphere is a very interesting region of the Earth's ionosphere. It is rich in various phenomena such as the Appleton F_2 region ionization anomaly, the *E* region equatorial electrojet, the F_2 region bubbles and the equatorial sporadic *E* layer. One of the most crucial factors that initiate and control all these ones is an electric field. On the basis of numerous observations, now it is well established [*Fejer*, 1986] that the average amplitude of the zonal component of equatorial electric field E_y ranges from 0.5 to 1.0 mV/m. During magnetically quiet periods the zonal electric field E_y is commonly eastward at daytime and westward at night; however, during magnetospheric disturbances the direction of E_y can be reversed. In the equatorial *E* region the zonal electric field E_y gives rise to a strong vertical polarization field E_z because electric conductivities at the lower and upper boundaries of the *E* layer are very small. If the E_y component is eastward, the E_z is directed up, and for the westward E_y the vertical electric field E_z is downward.

[3] As a result of combined acting of the zonal and vertical electric field components, a vertical drift of ions is set up in the *E* region. Calculations performed by *Raghavarao et al.* [1984] showed that the vertical ion drift produced by the electric field plays an important role in the nighttime equatorial *E* region, being noticeably modified a vertical ionization distribution. However, *Raghavarao et al.* [1984] simulated one particular situation that took place in the equatorial *E* region after the great geomagnetic storm of 8 March 1970 during a period of moderate geomagnetic activity on the night of 9–10 March 1970, as they used in their calculations a specific time variation of the zonal electric field E_y derived indirectly by *Goldberg et al.* [1974] by analysis of ionograms obtained from Thumba ($-1.7°$ magnetic dip), India, on the night of 9–10 March 1970, and furthermore, they used as an initial vertical profile of ion density the altitude distribution of N measured by *Goldberg et al.* [1974] in the evening of 9 March 1970.

[4] In the present paper we investigate the behavior of the nighttime *E* region over the magnetic equator during strong magnetospheric disturbances using the results of direct measurements of electric fields in the equatorial ionosphere reviewed by *Fejer* [1986] and *Fejer and Scherliess* [1997].

2. Formulation of Problem

2.1. Basic Equations

[5] Commonly, the major ionic constituents in the nighttime equatorial *E* region are molecular ions NO^+, O_2^+ and N_2^+, so the sum of their densities N is approximately equal to the electron density Ne, i.e., $N = N(NO^+) + N(O_2^+) + N(N_2^+) \approx Ne$. The ion density distribution can be obtained by solving the continuity equation for N. Taking into account that masses and collision frequencies of the ions NO^+, O_2^+, and N_2 are about the same, the continuity equation for their total density N can be written as

$$\frac{\partial N}{\partial t} + \mathrm{div}(N\mathbf{V}) = q - \alpha N^2, \tag{1}$$

where $\mathbf{V}$ is the ions' drift velocity, q the total nighttime production rate, and α the recombination quadratic coefficient.

[6] The ion drift velocity $\mathbf{V}$ has in general case terms due to electric fields, neutral winds, and diffusion. We shall assume that the ion drift is caused only by electric fields, any ion transport due to neutral winds and diffusion being neglected. In this case, the velocity of ion drift in the *E* region takes the form

$$\mathbf{V} = \mathbf{V_p} + \mathbf{V_h}, \tag{2}$$

0148-0227/02/2001JA900155$09.00

where $\mathbf{V_p}$ and $\mathbf{V_h}$ are Pedersen and Hall ion drift velocities, respectively. They can be written as

$$\mathbf{V_p} = \gamma_p \mathbf{E} \qquad \gamma_p = (e/m_i)\left[\nu_{in}/\left(\omega_i^2 + \nu_{in}^2\right)\right] \tag{3}$$

$$\mathbf{V_h} = \gamma_h \mathbf{E} \times \mathbf{B}/\mathrm{B} \qquad \gamma_h = (e/m_i)\left[\omega_i/\left(\omega_i^2 + \nu_{\mathrm{in}}^2\right)\right], \tag{4}$$

where e is an elementary charge, m_i the ion mass, ν_{in} the ion-neutral momentum transfer collision frequency, ω_i the ion gyrofrequency, and $\mathbf{E}$ and $\mathbf{B}$, the electric and geomagnetic fields, respectively. The transport term in the continuity equation (1) associated with Hall drift can be expanded as

$$\mathrm{div}(N\mathbf{V_h}) = N\mathrm{div}\mathbf{V_h} + (\mathbf{V_h} \cdot \mathrm{grad}\, N), \tag{5}$$

where

$$\mathrm{div}\mathbf{V_h} = \mathrm{div}(\gamma_h \mathbf{E} \times \mathbf{B}/B) = \gamma_h \mathrm{div}(\mathbf{E} \times \mathbf{B}/B) + ([\mathbf{E} \times \mathbf{B}/B] \cdot \mathrm{grad}\gamma_h). \tag{6}$$

Taking into account that

$$\mathrm{div}(\mathbf{E} \times \mathbf{B}/B) = [(\mathbf{B} \cdot \mathrm{curl}\, \mathbf{E}) - (\mathbf{E} \cdot \mathrm{curl}\, \mathbf{B})]/B + (\mathbf{E} \times \mathbf{B}) \cdot \mathrm{grad}(1/B) \approx 0, \tag{7}$$

one obtains

$$\mathrm{div}(N\,\mathbf{V_h}) = N(\mathbf{E} \times \mathbf{B}/B) \cdot \mathrm{grad}(e\gamma_h/m_i) + (e\gamma_h/m_i)[\mathbf{E} \times \mathbf{B}/B] \cdot \mathrm{grad}\, N = (\mathbf{E} \times \mathbf{B}/B) \cdot \mathrm{grad}(\gamma_h N). \tag{8}$$

[7] In the approximation of the horizontally stratified medium and horizontal geomagnetic field (the dip angle $I = 0°$), the continuity equation (1) accounting equations (2), (3), (4), and (8) takes the form

$$\frac{\partial N}{\partial t} + \frac{\partial}{\partial z}\left(\gamma_p N E_z\right) + E_y \frac{\partial}{\partial z}(\gamma_h N) = q - \alpha N, \tag{9}$$

where z is altitude and E_z and E_y are the upward and eastward components of E, respectively. If the zonal component of electric field E_y does not depend on altitude z, equation (9) can be rewritten as

$$\frac{\partial N}{\partial t} + \frac{\partial}{\partial z}(NV_z) = q - \alpha N^2, \tag{10}$$

where V_z is the vertical ion drift velocity, being the sum of vertical Pedersen drift velocity $V_{zp} = \gamma_p E_z$ and vertical Hall drift velocity $V_{zh} = \gamma_h E_y$, so that

$$V_z = \gamma_p E_z + \gamma_h E_y = (e/m_i)\left(\nu_{in} E_z + \omega_i E_y\right)/\left(\omega_i^2 + \nu_{in}^2\right). \tag{11}$$

Provided that there is no vertical current in the E region over the magnetic equator, the E_z and E_y components of electric field are related with each other as

$$E_z = (\sigma_2/\sigma_1)E_y, \tag{12}$$

where σ_1 and σ_2 are the Pedersen and Hall conductivities, respectively. Using the standard expressions for σ_1 and σ_2 yields

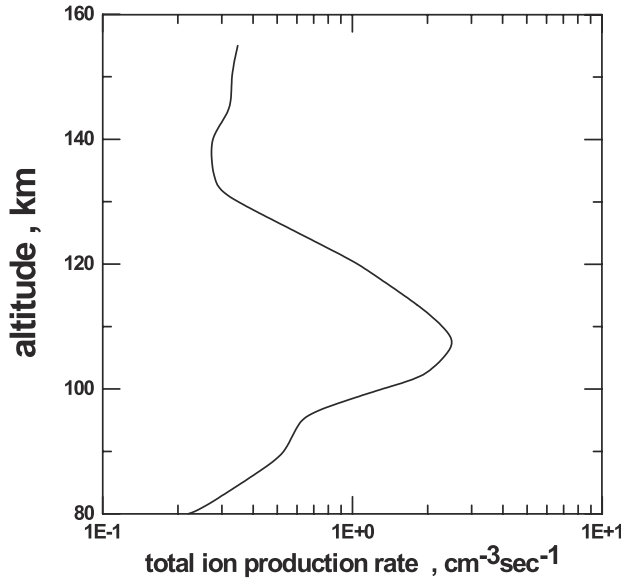

Figure 1. Total ion production rate versus altitude in the nighttime E region ionosphere. Read 1E-1 as 1×10^{-1}.

$$\sigma_2/\sigma_1 = \left\{\omega_e\left[\mathrm{m}_e\left(\omega_e^2 + \nu_{en}^2\right)\right]^{-1} - \omega_i\left[m_i\left(\omega_i^2 + \nu_{in}^2\right)\right]^{-1}\right\} \Big/ \left\{\nu_{en}\left[m_e\left(\omega_e^2 + \nu_{en}^2\right)\right]^{-1} + \nu_{in}\left[m_i\left(\omega_i^2 + \nu_{in}^2\right)\right]^{-1}\right\}, \tag{13}$$

where m_e is the electron mass, ν_{en} the electron-neutral momentum transfer collision frequency, and ω_e the electron gyrofrequency.

[8] It should be noted that as was shown first by *Untiedt* [1967] and then confirmed by *Sugiura and Poros* [1969], the vertical current in the E region over the dip equator is nonzero, and the relation between E_z and E_y differs from equation (12), however, as the estimates show, strictly over the dip equator there is quite a small difference in the altitude profiles of E_z obtained by *Untiedt* [1967] and *Sugiura and Poros* [1969], on one hand and given by equation (12), on the other hand, for the same altitude distributions of σ_1 and σ_2 and values of E_y.

[9] Substituting equations (12) into (11), one obtains

$$V_z = \left(e/m_i\right)\left[\left(\nu_{in}\sigma_2/\sigma_1 + \omega_1\right)/\left(\omega_i^2 + \nu_{in}^2\right)\right]E_y. \tag{14}$$

It is seen from equations (12), (13), and (14) that both E_z and V_z do not depend on the ion density.

[10] The continuity equation (10) can be solved numerically to give ion density as a function of altitude and time. The total nighttime ion production rate q (see Figure 1) includes the rates of ion production due to strong helium and hydrogen ultraviolet lines (H Lyman α 1216 Å, H Lyman β 1026 Å, He I 485 Å, and He Lyman α 304 Å) resonantly scattered on the geocorona [*Ogawa and Tohmatsu*, 1966; *Chen and Harris*, 1971]. The loss rate coefficient α is approximately equal to the dissociative recombination coefficient for $NO^+(\alpha_d(NO^+))$, which is given by $\alpha_d\,(NO^+) = 4.2 \times 10^{-7}\,(300/T_e)^{0.85}$ [*Walls and Dunn*, 1974]. For the ν_{in} and ν_{en} we adopted the expressions derived by *Schunk and Walker* [1973] and *Banks and Kockarts* [1973], respectively, using the neutral atmosphere model by *Jacchia* [1977] and the assumption that $T_i = T_e = T_n$.

2.2. Approximation of the Zonal Electric Field E_y

[11] The zonal electric field E_y is assumed to be independent with altitude, but it can undergo substantial time variations during magnetospheric disturbances [*Fejer*, 1986]. We consider two types

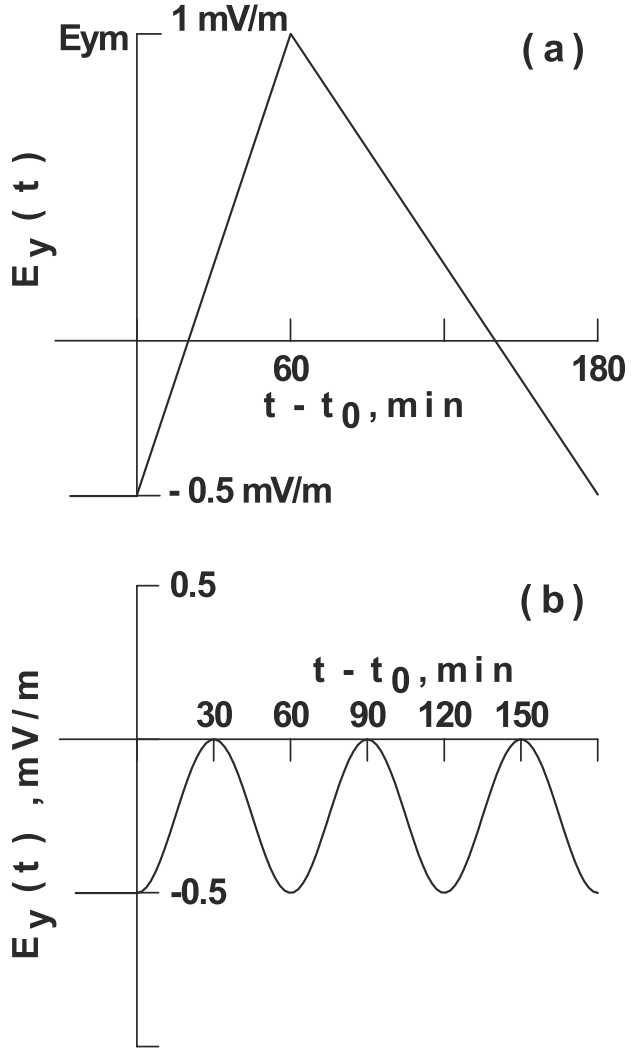

Figure 2. Adopted approximation of the zonal electric field E_y variations for (a) case 1 and (b) case 2.

of the E_y perturbations observed in the nighttime equatorial ionosphere, such as an rapid reversal of direction of E_y from westward to eastward and quasiperiodic time fluctuations of E_y being approximated for these two cases as follows:

$$E_y(t < t_0) = E_0 \tag{15a}$$

$$E_y(t_0 \le t \le t_0 + 60\ \text{min}) = E_0 + \left[\left(E_{ym} - E_0\right)(t - t_0)\right]/60 \tag{15b}$$

$$E_y(t_0 + 60\ \text{min} \le t \le t_0 + 180\ \text{min}) = E_{ym} - \left[\left(E_{ym} - E_0\right)(t - t_0 - 60)\right]/120 \tag{15c}$$

$E_0 = -0.5\text{mV/m}$, $E_{ym} = 0.5$ and 1mV/m.

Case 2

$$E_y(t < t_0) = E_0 \tag{16a}$$

$$E_y(t_0 \le t \le t_0 + 180\,\text{min}) = E_0\{\cos[2\pi(t - t_0)/T] + 1\}/2 \tag{16b}$$

$$E_0 = -0.5\text{mV/m}, T = 60\ \text{min}.$$

These approximations (see Figure 2) nearly fit the observed variations of E_y described by *Fejer* [1986] and *Fejer and Scherliess* [1997].

[12] We also performed a case study of ion density changes in the nighttime equatorial *E* region during the period of high substorm activity from 2300 LT on 7 March to 0500 LT on 8 March 1970 using an empirical model of storm time equatorial zonal electric field developed by *Fejer and Scherliess* [1997] (see Figure 8b) as there were no direct observations of E_y for this interval of local time.

2.3. Initial and Boundary Conditions

[13] As the initial condition (at $t \le t_0$), we treat the vertical profile of N obtained by solving the stationary continuity equation for N

$$\frac{\partial}{\partial z}(NV_z) = q - \alpha N^2 \tag{17}$$

assuming the zonal component of electric field E_y to be independent of time and westward with the value of -0.5 mV/m.

[14] At the lower boundary $z = 90$ km the ion density N is calculated using the continuity equation (10) that at this altitude can be written in the simplified form:

$$\frac{\partial}{\partial z}(NV_z) + N\frac{\partial V_z}{\partial z} = q - \alpha N^2. \tag{18}$$

The term $V_z(\partial N/\partial z)$ in equation (10) is neglected because as estimates show $|N(\partial V_z/\partial z)| \gg |V_z(\partial N/\partial z)|$ near $z = 90$ km.

3. Results

3.1. Vertical Ion Drift Velocity

[15] Figure 3 shows the calculated altitude profiles of Pedersen, Hall, and total vertical ion drift velocities and also vertical electric

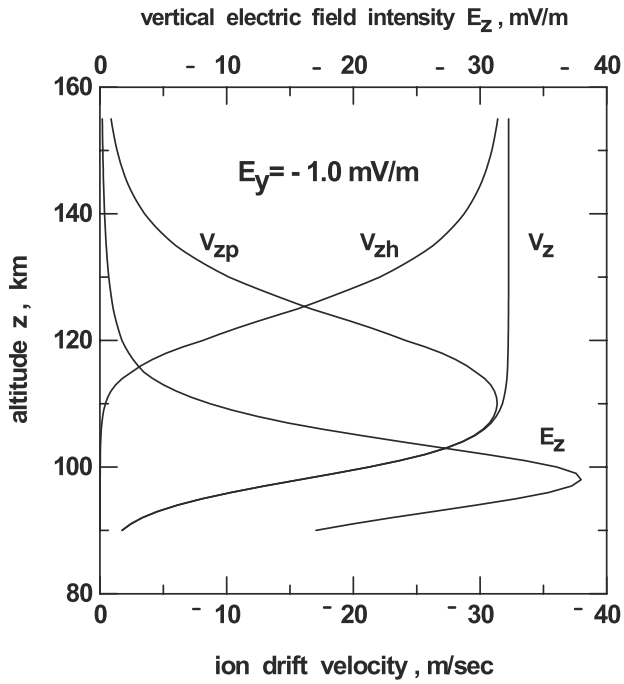

Figure 3. Altitude profiles of the vertical electric field E_z and Pedersen (V_{zp}), Hall (V_{zh}) and total ($V_z = V_{zp} + V_{zh}$) ion drift velocities in the nighttime *E* region over the magnetic equator for the zonal electric field $E_y = -0.001$ V/m.

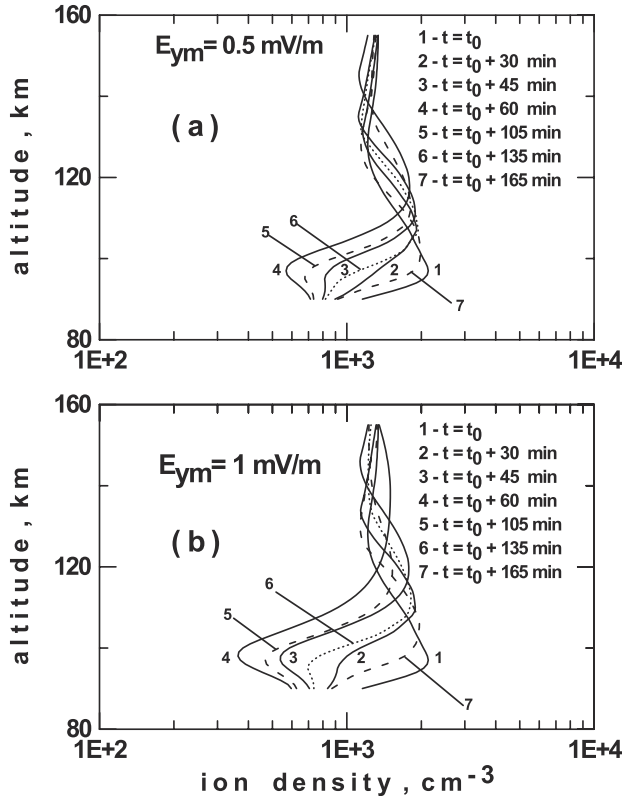

Figure 4. The calculated nighttime *E* region altitude ion density profiles over the magnetic equator for a magnetically quiet period (1) and at different time after a commencement of a rapid reversal of E_y associated with a strong magnetospheric substorm for (a) E_{ym} = 0.5 mV/m and (b) 1.0 mV/m (case 1).

field due to the westward zonal electric field (note that $E_y = -0.1$ mV/m). All the drift velocities and the vertical electric field E_z are downward. The maximum intensity of vertical electric field of ~37 mV/m is located at altitude near 98 km, which is substantially below the altitude of Pedersen mobility peak ($z_{pm} \sim 120$ km), that is why the Pedersen ion drift velocity attains its maximum at the noticeably lower altitude ($z \sim 110$ km) than the Pedersen mobility peak altitude. The total velocity of vertical ion drift rapidly increases with altitude up to ~110 km, being there approximately attained the value of velocity of electromagnetic $\mathbf{E} \times \mathbf{B}$ drift due to the zonal electric field E_y, and at altitudes above 120 km, it is practically independent of altitude.

3.2. Variations of Altitude Ion Density Profile

3.2.1. Case 1. [16] Figures 4a and 4b show the altitude profiles of computed ion density for the geomagnetically quiet period when the zonal electric field E_y is westward and does not depend on time and at different time after a commencement of rapid reversal of E_y direction associated with strong magnetospheric substorms for two values of the eastward electric field peak (E_{ym}) (E_{ym} = 0.5 mV/m (Figure 4a) and E_{ym} = 1.0 mV/m (Figure 4b)). The time variations of N_mE and H_mE are illustrated in Figure 5. It is seen that during a magnetically quiet period, the altitude ion density profile has a well-defined maximum ($N_mE \sim 2.1 \times 10^3$ cm^{-3}) at ~97 km. After the reversal of E_y direction to eastward, a strong modification of the altitude ion density profile occurs. Below 120 km, the altitude dependence of perturbed ion density is reverse with respect to that one corresponding to undisturbed conditions and instead of the *E* region maximum, the deep trough is formed at ~97 km. The minimum value of *N* within the trough is $\sim 5.0 \times 10^2$ cm^{-3} for E_{ym} = 0.5 mV/m and

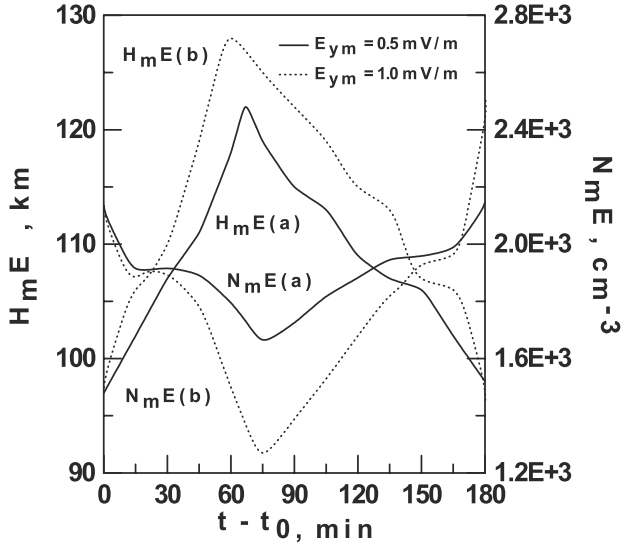

Figure 5. The time variations of N_mE and H_mE for case 1.

$\sim 3.0 \times 10^2$ cm^{-3} for E_{ym} = 1.0 mV/m, i.e., the ion density decreases by about a factor of 4 and 6, respectively. The *E* region maximum N_mE is lifted up by ~25 km for E_{ym} = 0.5 mV/m and by ~30 km for E_{ym} = 1.0 mV/m, being weakly expressed and amounted to 1.7×10^3 cm^{-3} for E_{ym} = 0.5 mV/m and to 1.3×10^3 cm^{-3} for E_{ym} = 1.0 mV/m. As a matter of fact, the *E* region is bifurcated into two layers with the major layer E_2 centered at ~120–125 km and the minor layer E_1 ($N_mE_1 \sim 5 \times 10^2$ cm^{-3}) centered at ~90 km.

3.2.2. Case 2. [17] Figure 6 depicts the time evolution of the ion density altitude profiles during a sequence of magnetospheric substorms when the zonal electric field component E_y undergoes quasiperiodical time fluctuations. Figure 7 shows the time variations of N_mE and H_mE. It is evident that when a magnitude of downward ion drift velocity decreases with time, the ion density maximum at 97 km decays, while at altitudes above 107 km, a new maximum of *N* starts to be formed. When the ion drift velocity

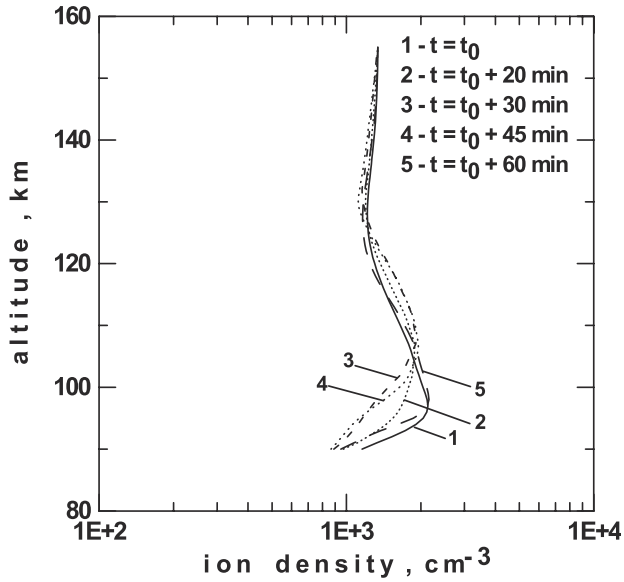

Figure 6. Same as Figure 3 but for quasiperiodical perturbations of E_y associated with a magnetospheric storm (case 2).

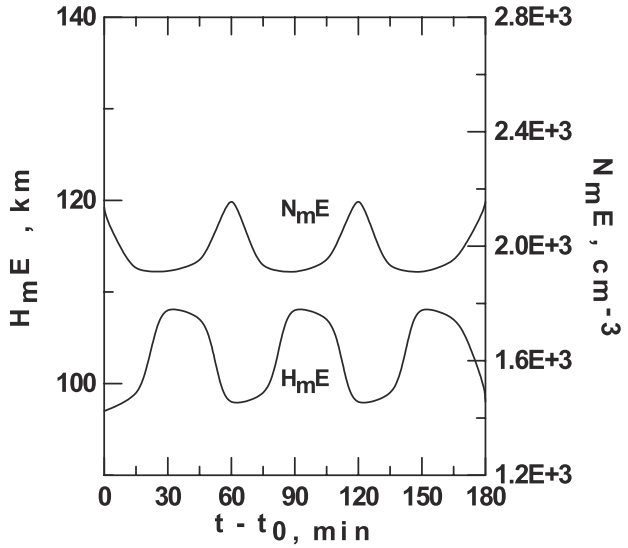

Figure 7. The time variations of N_mE and H_mE for case 2.

increases, the reverse situation occurs, i.e., the ion density rapidly increases in the lower *E* region and decreases in its middle part and the initial profile of *N* is restored. The most substantial changes of ion density take place in the lower *E* region at altitudes below 110 km, where *N* can decrease by a factor of 2. As can be seen from Figure 7, the values of N_mE and H_mE display quasiperiodical variations of the same period as that one of the E_y variations. The amplitude of N_mE variations is small and does not exceed 6% as

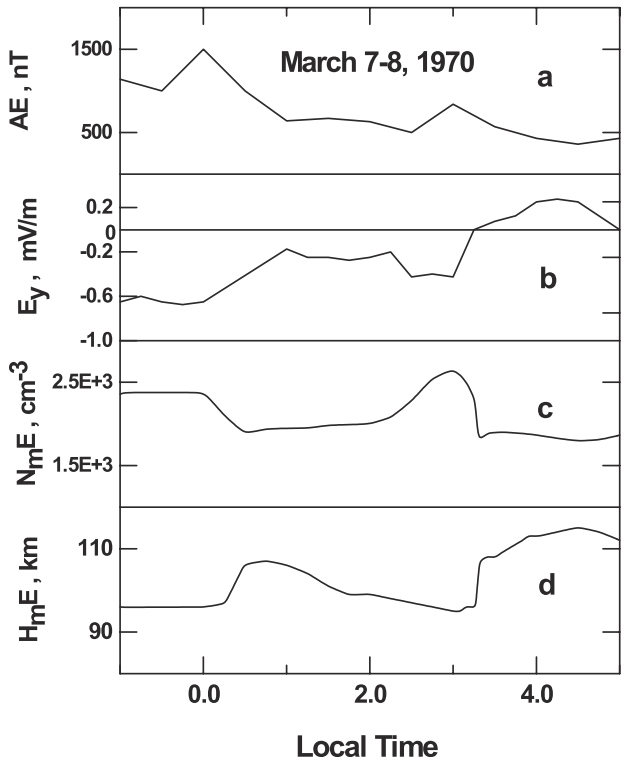

Figure 8. The local time variations of (a) the *AE* index, (b) the equatorial zonal electric field E_y obtained from the empirical model of E_y by *Fejer and Scherliess* [1997], (c) and (d) calculated values of N_mE and H_mE for the period from 2300 LT on 7 March to 0500 LT on 8 March 1970.

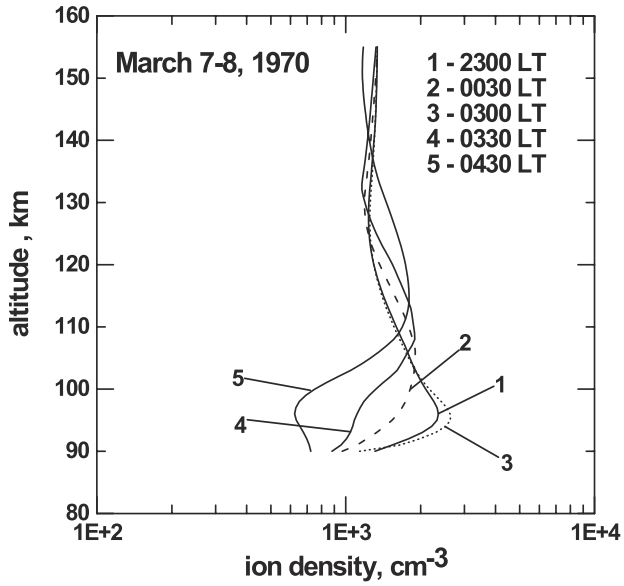

Figure 9. The calculated altitude ion density profiles in the nighttime equatorial *E* region at selected local times during the same period as Figure 8.

compared to the undisturbed value, but the changes of H_mE are quite noticeable being as large as 10 km.

3.2.3. Case study for the magnetically disturbed period of 7–8 March 1970. [18] Figure 8 shows, together with the local time variations in the auroral electrojet *AE* index (Figure 8a), the variations in the equatorial zonal electric field E_y obtained from an empirical model by *Fejer and Scherliess* [1997] (Figure 8b), the variations in the *E* region ion density peak value, N_mE (Figure 8c) and in the height of the *E* region peak, H_mE (Figure 8d) for the period from 2300 LT on 7 March to 0500 LT on 8 March 1970. We can see that from 2300 to 2400 LT on 7 March the equatorial zonal electric field is not perturbed and does not practically change with time having a typical quiet time value and westward direction although the *AE* indices showed moderate geomagnetic activity. On 8 March two successive enhancements of the *AE* index at ~0030 and 0300 LT were associated with eastward perturbations of E_y resulted in changes of N_mE and H_mE. It is seen that the variations of N_mE and H_mE are opposite to each other. In more details, behavior of the altitude distribution of ion density in the equatorial *E* region for the period considered is illustrated in Figure 9, which shows the altitude profiles of *N* at some selected times. Between 2300 and 0430 LT the altitude profile of *N* change in quasi-oscillatory manner proceeding the variations of the westward electric field magnitude, then 30 min after a reversal of direction of E_y from westward to eastward, a two layer structure of the equatorial *E* region is formed. At 0430 LT the altitude profile of ion density displays a deep trough at ~95 km where *N* is $\sim 6.0 \times 10^2$ cm^{-3}, i.e., the ion density decreased by about a factor of 4 relative to the value of *N* at 2300 LT.

4. Discussion and Summary

[19] In the present paper, a modeling study is made to simulate the nighttime equatorial *E* region ion density variations during strong magnetospheric disturbances due to perturbations of the zonal electric field E_y. The ion density *N* is calculated by solving the time-dependent continuity equation for ion density by assuming the time variations of E_y, which are fitted to some of the observed ones [*Fejer*, 1986; *Fejer and Scherliess*, 1997]. It is not our intention to discuss here what are the sources of the perturbations of E_y [*Raghavarao et al.*, 1984], but it is our goal to present

their possible effects on the *E* region. Electric fields affect the ion density due to producing a vertical ion drift that is composed, over the magnetic equator, of Pedersen and Hall components. The first one is determined by the vertical electric field component E_z and the other by E_y component. To derive E_z, we assumed that E_z is produced as a result of ionospheric plasma polarization due to the zonal electric field E_y, so that there is no vertical current in the *E* region over the magnetic equator. The altitude profile of vertical ion drift obtained in this paper differs from those calculated by *Hanson et al.* [1972] and *Raghavarao et al.* [1984] in that their profiles of V_z display pronounced peak at the altitude of maximum Pedersen mobility (z_{pm}), which exceeds the value of electromagnetic $\mathbf{E} \times \mathbf{B}$ drift by about a factor of 2, whereas our results indicate no peak in the altitude profile of V_z and that the value of V_z nowhere exceeds the $\mathbf{E} \times \mathbf{B}$ drift velocity being the saturation velocity for V_z. The difference between Hanson et al's and Radhavarao et al's and our results stems from the fact that instead of the relation between E_y and E_z, equation (12) resulting from the assumption that vertical current is equal to zero, they used for calculation of the vertical electric field E_z the methodology by *Sugiura and Poros* [1969]; however, in Sugiura and Poros's model the value of E_z at the level z_{pm} differs only by ~15% from the corresponding value of E_z following from the relation (12), while the values of E_z at z_{pm} altitude calculated by *Hanson et al.* [1972] and *Raghavarao et al.* [1984] are more than three times as large as that one resulting from equation (12).

[20] As reviewed by *Fejer* [1986], during severe magnetospheric substorms and storms a variety of large perturbations of the zonal electric field E_y has been observed in the equatorial ionosphere. They can last from a few minutes to a few hours at all longitudes. The magnitude of the equatorial electric field perturbations is the largest in the midnight-sunrise period. As an input for our model calculations of the *E* region ion density variations, we considered two types of the observed nighttime perturbations of E_y: a rapid reversal of E_y direction from westward to eastward that can occur during a strong substorm and quasiperiodical time variations magnitude of E_y observed during a magnetospheric storm. Also, we used an empirical model of disturbed equatorial zonal electric field by *Fejer and Scherliess* [1997] to carry out a case study of the changes in the nighttime equatorial *E* region during the period of long-lasting substorm activity on 7–8 March 1970.

[21] While solving the continuity equation, assumptions were made that all quantities envolved can spatially change only with altitude *z* (horizontal stratification approach), the value of zonal electric field E_y is independent of *z* and the *E* region ion population are only molecular ions NO^+, O_2^+, and N_2^+, so that no metallic ions are included into consideration. The assumptions are quite reasonable for the dip angle *I* range $-1.5°$ to $+1.5°$.

[22] The results of calculations indicate that during strong magnetospheric disturbances the altitude structure of the nighttime equatorial *E* region is substantially modified, with the largest effects in the lower part of *E* region ($z < 105$ km), where a deep trough in ion density is formed instead of the quiet *E* region maximum. The ion density in the trough is ~1/6 times the undisturbed value of *N*. The *E* region maximum N_mE can be lifted up by ~30 km, being ~2× decreased as compared with the quiet time value of N_mE. In the course of the magnetospheric disturbance the *E* region is bifurcated into two layers.

[23] It is interesting to note that the deep trough of ion density in the lower *E* region over the magnetic equator represents, in fact, a duct for LF and VLF electromagnetic waves, so that during magnetospheric disturbances, the favorable conditions arise for the LF and VLF radio wave propagation along the magnetic equator.

[24] **Acknowledgments.** The authors would like to thank the referees for very useful comments and suggestions that have improved this paper. We are also thankful to G. S. Lakhina for his encouragement.

[25] Hiroshi Matsumoto thanks A. W. Wernik and another referee for their assistance in evaluating this paper.

References

Banks, P., and G. Kockarts, *Aeronomy*, part B, 355 pp., Academic, San Diego, Calif., 1973.

Chen, W. M., and R. D. Harris, An ionospheric *E*-region nighttime model, *J. Atmos. Terr. Phys.*, *33*, 1193–1207, 1971.

Fejer, B. G., Equatorial ionospheric electric fields associated with magnetospheric disturbances, in *Solar Wind-Magnetosphere Coupling*, edited by Y. Kamide, and J. A. Slavin, pp. 519–545, Terrupub, Tokyo, 1986.

Fejer, B. G., and L. Scherliess, Empirical models of storm time equatorial zonal electric fields, *J. Geophys. Res.*, *102*, 24,047–24,056, 1997.

Goldberg, R. A., A. C. Aikin, and B. V. Krishnamurthy, Ion composition and drift observations in the nighttime equatorial ionosphere, *J. Geophys. Res.*, *79*, 2473–2477, 1974.

Hanson, W. B., D. L. Sterling, and R. F. Woodman, Source and identification of heavy ions in the equatorial *F* layer, *J. Geophys. Res.*, *77*, 5530–5541, 1972.

Jacchia, L. G., Thermospheric temperature, density and composition: New models, *Smithson. Astrophys. Obs. Spec. Rep.*, *375*, 1977.

Ogawa, T., and T. Tohmatsu, Photoelectronic processes in the upper atmosphere, II, The hydrogen and helium ultraviolet glow as an origin of the nighttime ionosphere, *Rep. Ionos. Space Res. Jpn.*, *20*, 395–417, 1966.

Raghavarao, R., R. Sridharan, and R. Suhasini, The importance of vertical ion currents on the nighttime ionization in the equatorial electrojet, *J. Geophys. Res.*, *89*, 11,033–11,037, 1984.

Schunk, R. W., and J. C. G. Walker, Theoretical ion densities in the lower ionosphere, *Planet. Space Sci.*, *21*, 1875–1896, 1973.

Sugiura, M., and D. J. Poros, An improved model: Equatorial electrojet with a meridional current system, *J. Geophys. Res.*, *74*, 4025–4034, 1969.

Untiedt, J., A model of the equatorial electrojet involving meridional currents, *J. Geophys. Res.*, *72*, 5799–5810, 1967.

Walls, F. L., and G. H. Dunn, Measurement of total cross sections for electron recombination with NO^+ and O_2^+ using ion storage techniques, *J. Geophys. Res.*, *79*, 1911–1915, 1974.

V. V. Hegai and V. P. Kim, Institute of Terrestrial Magnetism, Ionosphere and Radio Wave Propagation (IZMIRAN), Troitsk, Moscow Region, 142190, Russia. (kimvp@izmiran.rssi.ru; hegai@izmiran.rssi.ru)

M. Lal, Equatorial Geophysical Research Laboratory, Indian Institute of Geomagnetism, Krishnapuram, Tirunelveli 627011, India. (moegrl@iig.iigm.res.in)